

The influence of surface tension in thin-film hydrodynamics: gravity free planar hydraulic jumps.

Rajesh K Bhagat¹

¹Department of Applied Mathematics and Theoretical Physics, Wilberforce Road, Cambridge, the UK

Corresponding author: rkb29@cam.ac.uk

(Received xx; revised xx; accepted xx)

Hydraulic jumps in thin films are traditionally explained through gravity-driven shallow-water theory, with surface tension assumed to play only a secondary role via Laplace pressure. Recent experiments, however, suggest that surface tension can be the primary mechanism. In this work we develop a theoretical framework for *surface-tension-driven hydraulic jumps* in planar thin-film flows. Starting from the full interfacial stress conditions, we show that the deviatoric component of the normal stress enters at leading order and fundamentally alters the balance. A dominant-balance analysis in the zero-gravity limit yields parameter-free governing equations, which admit a similarity solution for the velocity profile. Depth-averaged momentum conservation then reveals a singularity at unit Weber number, interpreted as the criterion for hydraulic control. This singularity is regularised by a non-trivial pressure gradient at the jump. This work establishes the theoretical basis for surface-tension-driven hydraulic jumps, providing analytical predictions for the jump location and structure.

Key words: Thin films; Hydraulic jump; Surface tension; Capillary flows

1. Introduction

Recently, the role of surface tension in hydrodynamics—particularly for kitchen-sink-scale hydraulic jumps—has been debated Bhagat *et al.* (2018, 2020); Bhagat & Linden (2020); Duchesne & Limat (2022). These jumps, documented since Leonardo da Vinci (Marusic & Broomhall 2021), are classically attributed to gravity. In large-scale open-channel flows, the depth-averaged inviscid (Saint–Venant) equations are hyperbolic, and a hydraulic jump can be interpreted as a shock-like transition connecting supercritical and subcritical states, with criticality associated with the long-wave gravity-wave speed. In the radial setting, however, Bohr *et al.* showed that the ideal (inviscid) shallow-water equations do not allow a determination of the jump position (Bohr *et al.* 1993).

Applying this wave-propagation argument to viscous thin films is theoretically ambiguous. The viscous shallow-water equations used to describe these flows are not hyperbolic;

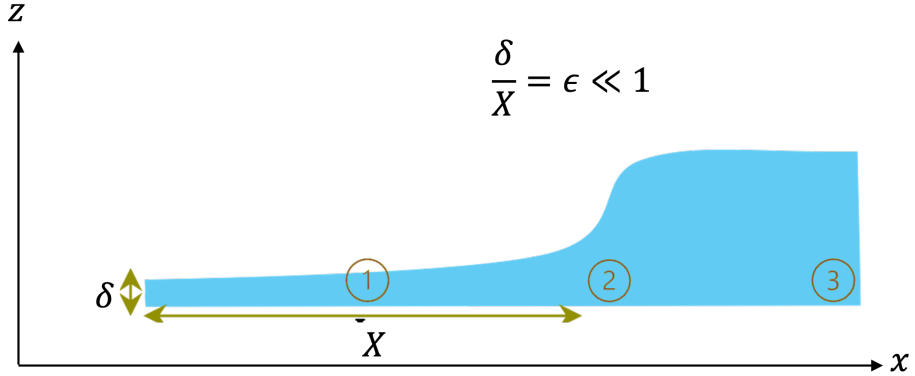


Figure 1. Planar hydraulic-jump geometry.

instead, they contain a parabolic contribution arising from wall shear stress, which plays a key role in setting the dynamics (Watson 1964; Bohr *et al.* 1993). Consequently, the system does not admit the same characteristic-based notion of information propagation as in the inviscid theory. Nevertheless, Jannes & Rousseaux (2012) provided experimental evidence supporting the supercritical/subcritical interpretation in a thin film using *silicone* oil. Via Mach-cone measurements, they demonstrated unidirectional propagation of surface disturbances in the fast-moving film and identified the hydraulic jump as a sharp boundary separating super- and subcritical regimes. Physically, this is consistent with viscous stresses decelerating the flow while the film thickens: the long-wave gravity-wave speed increases whereas the mean speed decreases, driving the Froude number toward criticality and leading to choking and the jump. A complementary view, developed by Kurihara (1946); Tani (1949), attributes the jump to boundary-layer separation driven by an adverse gravitational pressure gradient that builds up as the film thickens.

Bhagat *et al.* (2018) challenged the classical picture and proposed a surface-tension–driven mechanism. They argued that hydraulic jumps may be controlled by surface tension, gravity, or a combination of both, and suggested a composite criticality condition based on an energy balance,

$$\text{We}^{-1} + \text{Fr}^{-2} = 1, \quad (1.1)$$

where the local Froude and Weber numbers are defined as

$$\text{Fr}^2 = \frac{2\bar{u}^2}{gh}, \quad \text{We} = \frac{\rho \bar{u}^2 h}{\sigma}.$$

Here u is the velocity, h is the local film thickness, ρ is the density, and σ is the surface tension. In thin films they further argued that gravity can be subdominant ($\text{Fr} \gg 1$), so that surface tension provides the dominant control.

While much of the debate has centred on circular jumps, the fundamental balance between surface tension and gravity remains unresolved. To separate physical mechanisms from geometric effects, we consider steady, planar, thin-film channel flow. Under conventional shallow-water scalings—normalising the pressure either by a dynamic scale (kinetic-energy density) or by hydrostatics—the leading-order balances are hydrostatic in the wall-normal direction and viscous–gravity in the streamwise direction Balmforth & Mandre (2004); Dhar *et al.* (2020); Razis *et al.* (2021). For nearly flat films, this would suggest that surface tension does not enter at leading order.

We challenge that inference. We show that, beyond the Laplace pressure, the deviatoric normal stress can enter the leading-order balance and, in a zero-gravity thin-film regime, control the dynamics. We first analyse the zero-gravity limit and develop a theoretical framework for surface-tension–driven hydraulic control and jumps, and then validate the predictions against numerical simulations.

The paper is organised as follows. Section 2 interprets criticality via a capillary–gravity wave argument. Section 3 states the governing equations and boundary conditions, derives the interfacial conditions without *a priori* assumptions, and scales them to identify the leading-order terms. Section 4 develops the asymptotics: a dominant-balance analysis identifies the characteristic scales and yields a parameter-free system, from which a similarity solution and a depth-integrated momentum equation are obtained. The latter exhibits a singularity at a unit *effective* local Weber number, which is regularised by pressure. Section 6 summarises the findings.

2. Hydraulic jump as a zero-mode standing wave

We frame the steady hydraulic jump as a *wave-pinning* problem: a location where a surface wave propagating against the flow is held stationary by the background current. In this sense, the jump may be viewed as a *standing wave* in the laboratory frame (a *zero-mode*, $\omega = 0$) of the gravity-capillary dispersion relation. Using silicone oil as the working fluid, Jannes & Rousseaux (2012) performed Mach cone experiments and identified subcritical and supercritical regions separated by the jump, consistent with a blocking point where the background flow first matches the relevant long-wave propagation speed.

For small free-surface disturbances on a layer of depth h with a uniform current U in the streamwise direction, the Doppler-shifted dispersion relation is

$$(\omega - kU)^2 = \left(gk + \frac{\sigma}{\rho} k^3 \right) \tanh(kh), \quad \mathcal{Q} := \omega - kU, \quad (2.1)$$

where ω and k are the laboratory-frame frequency and wavenumber, and \mathcal{Q} is the intrinsic (fluid-frame) frequency.

2.1. Gravity-induced jump: setting $\sigma = 0$

In the absence of surface tension and in the shallow-water limit ($kh \ll 1$), (2.1) reduces to $(\omega - kU)^2 \simeq gh k^2$, i.e. a non-dispersive relation with phase and group speeds equal to $c = \sqrt{gh}$. A steady (zero-mode) standing wave requires $\omega = 0$, hence $\mathcal{Q} = -kU$ and $U = |\mathcal{Q}/k| = c = \sqrt{gh}$, which yields the classical criterion

$$U^2 = gh \iff \text{Fr}^2 = 1, \quad (2.2)$$

with $\text{Fr} := U/\sqrt{gh}$.

2.2. Surface-tension (capillary)-induced jump: setting $g = 0$

The capillary part of (2.1) is dispersive: the intrinsic phase speed $c_{p0}(k) = \mathcal{Q}/k$ increases with k . In *deep water* ($kh \gg 1$) this scales as $c_{p0} \sim \sqrt{(\sigma/\rho)k}$ and therefore becomes unbounded as $k \rightarrow \infty$. If one considers arbitrarily short capillary ripples, this appears to imply that for any given mean flow U there always exists a sufficiently short wave that can propagate upstream, so the flow would never be truly “supercritical” with respect to *all* capillary modes.

The resolution is that hydraulic control concerns depth-averaged communication of mass and momentum. Only *long* waves (in the shallow-water sense) have a substantial depth-

The Influence of surface tension in hydrodynamics

integrated signature; very short capillary ripples are confined to a thin interfacial layer and are strongly damped by viscosity. Accordingly, we restrict attention to the *long-wave* band

$$S = \{ k : 0 < kh \leq \psi \}, \quad \psi = O(1), \quad (2.3)$$

where the dimensionless cutoff ψ serves as an *effective* upper limit for hydraulically relevant waves. Besides the formal shallow-water validity ($kh \lesssim \psi_{\text{sw}}$), practical limits arise from (i) *excitation*: the background inhomogeneity of length L injects little energy at $k \gg 1/L$ (so $\psi_{\text{exc}} \sim h/L$), and (ii) *dissipation*: high- k waves are strongly damped (viscous decay $\gamma \sim 2\nu k^2$), giving an attenuation length $\ell_{\text{damp}} \approx c_g^{\text{lab}}/(2\nu k^2)$ that falls rapidly with k . Modes with ℓ_{damp} shorter than a few wavelengths do not contribute to a steady state. We therefore take

$$\psi = \min\{\psi_{\text{sw}}, \psi_{\text{exc}}, \psi_{\text{diss}}\}$$

and treat it as an $O(1)$ constant to be fixed by the flow configuration. Typically ψ_{exc} and ψ_{diss} exceed unity (see Appendix 1), so the effective cutoff is often set by the shallow-water limit and we may take $\psi = \psi_{\text{sw}}$.

Isolating capillarity by setting $g = 0$, the dispersion relation is

$$\Omega^2 = \left(\frac{\sigma}{\rho} k^3 \right) \tanh(kh), \quad c_{p0}(k) = \frac{\Omega}{k} = \sqrt{\frac{\sigma}{\rho} k \tanh(kh)}. \quad (2.4)$$

A *zero-mode* (standing wave in the laboratory frame) is obtained by imposing $\omega = 0$, which gives $\Omega = -kU$ and therefore the phase-speed matching condition

$$U = c_{p0}(k) \iff U^2 = \frac{\sigma}{\rho} k \tanh(kh). \quad (2.5)$$

Within the admissible long-wave band S , $c_{p0}(k)$ monotonically increases with k , so the *last* steady long wave to survive is the *fastest* admissible long wave at the band edge $k_{\text{max}} = \psi/h$. Evaluating (2.5) at k_{max} yields the edge-of-band threshold

$$U_{\text{crit}}^2 = \frac{\sigma}{\rho} \frac{\psi}{h} \tanh \psi, \quad (g = 0, \text{ steady zero-mode}). \quad (2.6)$$

We define the local *wave-Weber* number based on the band-edge wavenumber $k_{\text{max}} = \psi/h$,

$$\text{We} := \frac{\rho U^2 h}{\sigma \psi^2}, \quad (2.7)$$

for which (2.6) becomes

$$\text{We}_{\text{crit}}^{(\text{steady})} = \frac{\tanh \psi}{\psi}.$$

(2.8)

Thus, at $g = 0$, a steady capillary-controlled jump occurs when U equals the phase speed of the fastest admissible long capillary wave ($k = \psi/h$).

2.3. Gravity-capillary induced jump (completed picture)

Combining gravity and surface tension in the *steady* setting, we use the zero-mode condition $\omega = 0$ and the admissible long-wave band $0 < kh \leq \psi$ to obtain

$$U_{\text{crit}}^2 = \left(\frac{gh}{\psi} + \frac{\sigma}{\rho} \frac{\psi}{h} \right) \tanh \psi \quad \Rightarrow \quad \frac{1}{\text{Fr}^2} + \frac{1}{\text{We}} = \frac{\psi}{\tanh \psi} \approx 1,$$

(2.9)

where $\text{Fr} := U/\sqrt{gh}$ and We is defined in (2.7). Criticality corresponds to satisfying (2.9). Rearranging (2.9) yields

$$\boxed{\text{Fr}^2 \approx 1 + \frac{1}{\text{Bo}}}, \quad (2.10)$$

with the Bond number defined as

$$\text{Bo} := \frac{\rho gh^2}{\sigma \psi^2} = \frac{h^2}{\psi^2 l_c^2}, \quad l_c := \sqrt{\frac{\sigma}{\rho g}}. \quad (2.11)$$

Thus, for $\text{Bo} \gg 1$ (thick films, $h \gg \psi l_c$) the jump is *gravity-controlled* with $\text{Fr} \approx 1$; whereas for $\text{Bo} \ll 1$ (thin films) the capillary term sets the threshold, which is equivalently captured by $\text{We} \approx 1$.

This standing wave viewpoint shows that capillarity can, in principle, set hydraulic control even within an inviscid wave-propagation framework.

3. Theory

We derived the composite criterion for the thin-film hydraulic jump by interpreting the jump as a steady ('zero-mode') standing wave. We now examine the role of surface tension in such films—a point of recent debate—using momentum equation and quantify the conditions under which capillarity, rather than gravity, sets the control.

We consider a 2-D, steady, incompressible, Newtonian thin film with constant properties. Gravity is set to zero in this section to expose the mechanism cleanly. Cartesian coordinates are used with x streamwise and z wall-normal; the velocity is $\mathbf{u} = (u, w)$. The volumetric flux per unit span is

$$Q = \int_0^{h(x)} u(x, z) dz. \quad (3.1)$$

The steady incompressible governing equations (in conservative form) are

$$\partial_x u + \partial_z w = 0, \quad (3.2)$$

$$u \partial_x(u) + w \partial_z(u) = -\frac{1}{\rho} \partial_x p + \nu(\partial_{xx} u + \partial_{zz} u), \quad (3.3)$$

$$\partial_x(uw) + \partial_z(w^2) = -\frac{1}{\rho} \partial_z p + \nu(\partial_{xx} w + \partial_{zz} w), \quad (3.4)$$

where ν is the kinematic viscosity.

3.1. Interface geometry and boundary conditions

We define the free surface by $J(x, z) = z - h(x) = 0$ (Bush & Aristoff 2003). The unit normal and tangent to the free surface are

$$\mathbf{n} = \frac{1}{\sqrt{1 + h'^2}} \begin{bmatrix} -h' \\ 1 \end{bmatrix}, \quad \mathbf{t} = \frac{1}{\sqrt{1 + h'^2}} \begin{bmatrix} 1 \\ h' \end{bmatrix}, \quad (3.5)$$

and the curvature is

$$\kappa = \nabla \cdot \mathbf{n} = -\frac{h''}{(1 + h'^2)^{3/2}}.$$

We denote the rate-of-strain tensor by

$$e_{ij} = \frac{1}{2}(\partial_i u_j + \partial_j u_i)$$

and the Cauchy stress by

$$\mathbf{T} = -p \mathbf{I} + 2\mu \mathbf{e}$$

with the dynamic viscosity $\mu = \rho\nu$. We apply no slip and no penetration condition at the wall ($z = 0$):

$$\text{at the wall: } (z = 0) \quad u = 0; \quad w = 0. \quad (3.6)$$

We assume a clean interface, and negligible gas shear and hence the boundary condition at the free surface $z = h(x)$. The boundary conditions are,

$$\text{kinematic: } w = u_s h', \quad \text{where, } u_s(x) := u(x, h), \quad (3.7a)$$

$$\text{zero tangential stress: } \mathbf{t} \cdot \mathbf{e} \cdot \mathbf{n} = 0, \quad (3.7b)$$

$$\text{normal stress with surface tension: } -p + 2\mu \mathbf{n} \cdot \mathbf{e} \cdot \mathbf{n} = -\sigma \kappa. \quad (3.7c)$$

For an analytical solution we resolve (3.7b) and (3.7c) further.

3.1.1. Zero tangential stress

Resolved along $x - z$ using (3.5), (3.7b) becomes

$$\left[\frac{1 - h'^2}{1 + h'^2} (\partial_z u + \partial_x w) + \frac{2h'}{1 + h'^2} (\partial_z w - \partial_x u) \right]_{z=h} = 0. \quad (3.8)$$

Note that the streamwise axis x is generally *not* aligned with the free-surface tangent. The zero-tangential-stress condition applies along the surface tangent \mathbf{t} , not along x . Consequently, its projection onto the x -direction does *not* enforce $\partial_z u = 0$ at $z = h$; a small residual streamwise shear is permitted. In the long-wave regime ($|h'| = O(\epsilon)$), this shear is $O(\epsilon^2)$ and is negligible at leading order. For completeness—and to keep the analysis explicit—we retain all terms below and discard the $O(\epsilon^2)$ contribution only when taking the leading-order limit. Solving (3.8) for the streamwise shear at the free surface $(\partial_z u + \partial_x w)$ gives

$$\begin{aligned} (\partial_z u + \partial_x w)|_{z=h} &= -\frac{2h'}{1 - h'^2} (\partial_z w - \partial_x u) \\ &= \frac{4h'}{1 - h'^2} \partial_x u \quad (\text{using continuity } \partial_z w = -\partial_x u). \end{aligned} \quad (3.9)$$

Equations (3.8)–(3.9) are *exact* for any slope $|h'| < 1$ (the long-wave regime).

3.1.2. Normal stress condition

The deviatoric component of normal stress is resolved to

$$n_i e_{ij} n_j = \frac{1}{1 + h'^2} \left[(h')^2 \partial_x u - h' (\partial_z u + \partial_x w) + \partial_z w \right]_{z=h}, \quad (3.10)$$

which, using (3.9) and continuity, reduces to

$$\boxed{n_i e_{ij} n_j = -\frac{1 + h'^2}{1 - h'^2} \partial_x u \Big|_{z=h} = \frac{1 + h'^2}{1 - h'^2} \partial_z w \Big|_{z=h}}. \quad (3.11)$$

For nearly flat films ($|h'| \ll 1$) this simplifies to

$$\boxed{n_i e_{ij} n_j \Big|_{z=h} \rightarrow \partial_z w \Big|_{z=h} = -\partial_x u \Big|_{z=h}}. \quad (3.12)$$

Thus, even at leading order, the deviatoric component of normal stress contribute to the normal stress balance; only in the inviscid limit $\mu \rightarrow 0$ removes this contribution, leaving Laplace pressure only.

3.2. Scaling

Here we will first carry out a generic nondimensionalisation and later identify the characteristic scales by a dominant-balance argument. Introduce characteristic scales

$$x = X x^*, \quad z = \delta z^*, \quad h = \delta h^*, \quad u = \nu u^*, \quad w = \frac{\delta \nu}{X} w^*,$$

where δ is the characteristic film thickness, X the streamwise length scale, and ν the velocity scale, and the aspect ratio

$$\epsilon \equiv \frac{\delta}{X} \ll 1.$$

In zero gravity free surface flow, pressure should naturally be scaled with capillary pressure; with $\kappa \sim \delta/X^2$ we set:

$$p = \frac{\sigma \delta}{X^2} p^*.$$

Define the Reynolds and Weber numbers

$$Re = \frac{\nu \delta}{\nu}, \quad We = \frac{\rho \nu^2 \delta}{\sigma}.$$

For notational convenience, we now drop the asterisks; all variables below are dimensionless unless stated otherwise. Dropping asterisks, the nondimensional equations are

$$\partial_x u + \partial_z w = 0, \tag{3.13}$$

$$\partial_x(u^2) + \partial_z(uw) = -\frac{\epsilon^2}{We} \partial_x p + \frac{\epsilon}{Re} \partial_{xx} u + \frac{1}{\epsilon Re} \partial_{zz} u, \tag{3.14}$$

$$\partial_x(uw) + \partial_z(w^2) = -\frac{1}{We} \partial_z p + \frac{\epsilon}{Re} \partial_{xx} w + \frac{1}{\epsilon Re} \partial_{zz} w. \tag{3.15}$$

The (dimensionless) flux is

$$\int_0^h u \, dz = F, \quad F \equiv Q/(\nu \delta). \tag{3.16}$$

3.2.1. Scaled boundary condition

At the wall, we have $u = 0$; $w = 0$, and the kinematic condition at free surface is $w = u_s h'$. The resolved tangential condition (3.8) yields, to $\mathcal{O}(\epsilon^2)$,

$$\partial_z u = -\epsilon^2 \left[\partial_x w + \frac{2h'}{1 - \epsilon^2 h'^2} (\partial_z w - \partial_x u) \right]_{z=h}, \tag{3.17}$$

so the streamwise free-surface shear is $\mathcal{O}(\epsilon^2)$. The normal-stress condition gives

$$-\frac{p}{We} + \frac{2}{\epsilon Re} \partial_z w = \frac{h''}{We} + \mathcal{O}(\epsilon^2) \quad (z = h). \tag{3.18}$$

Writing the free-surface conditions in this resolved, scaled form exposes the hierarchy in ϵ, Re, We and allows direct substitution into depth-integrated balances.

4. Asymptotic analysis for the critical regime

4.1. Critical-regime scales (capillary control)

We now determine the characteristic scales (X, δ, ν) by dominant balances: 1) mass conservation, 2) inertia viscous balance, and 3) capillary control, appropriate to the critical regime:

$$\text{mass conservation:} \quad Q \sim \nu \delta, \quad (4.1)$$

$$\text{inertia-viscous balance:} \quad u \partial_x u \sim \nu \partial_{zz} u \Rightarrow \nu \delta^2 \sim \nu X, \quad (4.2)$$

$$\text{capillary control:} \quad \text{We} = \mathcal{O}(1) \Rightarrow \rho \nu^2 \delta \sim \sigma. \quad (4.3)$$

Solving (4.1)–(4.3) for (X, δ, ν) yields the unique scales

$$X = \frac{Q^3 \rho}{\sigma \nu}, \quad \delta = \frac{Q^2 \rho}{\sigma}, \quad \nu = \frac{\sigma}{\rho Q}. \quad (4.4)$$

Hence,

$$Re = \frac{Q}{\nu} = \epsilon^{-1} \quad \text{so} \quad \epsilon Re = 1, \quad \text{and} \quad We = 1, \quad (4.5)$$

4.2. Parameter-free leading-order system

With (4.5) inserted in (3.13)–(3.15) and retaining the dominant long-wave terms and ignoring $\mathcal{O}(\epsilon^2)$ terms, the governing equations reduce to

$$\partial_x u + \partial_z w = 0, \quad (4.6)$$

$$u \partial_x u + w \partial_z u = \partial_{zz} u, \quad (4.7)$$

$$\partial_x(uw) + \partial_z(w^2) = -\partial_z p + \partial_{zz} w, \quad (4.8)$$

the dimensionless flux reduces to

$$\int_0^h u \, dz = 1, \quad F \equiv Q/(\nu \delta) = 1, \quad (4.9)$$

and the boundary conditions simplifies to

$$u = w = 0 \quad (z = 0), \quad (4.10)$$

$$w = u_s h', \quad (z = h), \quad (4.11)$$

$$\partial_z u = 0 \quad (z = h), \quad (4.12)$$

$$-p + 2 \partial_z w = h'' \quad (z = h). \quad (4.13)$$

4.3. Similarity solution and depth-averaged relations

Guided by the leading order streamwise momentum equation (4.7) and the boundary conditions (4.10) and (4.11), we adopt a planar similarity profile,

$$u(x, z) = u_s(x) f(\eta), \quad \eta = \frac{z}{h(x)}, \quad (4.14)$$

with $f(0) = 0, f(1) = 1, f'(1) = 0$. The flux constraint gives

$$\int_0^h u \, dz = 1 \Rightarrow u_s h I_1 = 1, \quad I_1 := \int_0^1 f(\eta) \, d\eta. \quad (4.15)$$

From the flux constraint (4.15) we have $u_s h = \text{constant}$. Using continuity (4.6) with the ansatz (4.14) then yields,

$$w(x, z) = u_s(x) h'(x) \eta f(\eta). \quad (4.16)$$

Substituting (4.14)–(4.16) into the streamwise momentum equation (4.7) and using ($u_s h = \frac{1}{I_1} = \text{const}$) yields a separated equation

$$h^2 \frac{du_s}{dx} = \frac{f''(\eta)}{f(\eta)^2} := -\frac{3}{2}c^2 \quad (4.17)$$

Note $f''(\eta) \leq 0$ as the shear stress is maximum at the plate, and $f'(1) = 0$, and the right-hand side is a constant by separation. Equation (4.17) gives the same shape function as obtained by Watson (1964) for an axisymmetric boundary layer flow, and the shape function can be obtained by setting,

$$\begin{aligned} \frac{f''(\eta)}{f^2(\eta)} &= -\frac{3}{2}c^2 \\ \implies f'^2 &= c^2(1 - f^3) \end{aligned} \quad (4.18)$$

Equation (4.18) can be integrated to obtain the shape factor. Since $f' \geq 0$, and $f(1) = 1$, we can get $c = 1.402$, similarly $I_1 = 0.615$ are the same as Watson (1964) due to same shape ODE. Using $u_s h = 1/I_1$, differentiating and combining with (4.17) gives a constant free-surface slope

$$u_s h \frac{dh}{dx} = \text{constant} = \frac{3}{2}c^2 \quad (4.19)$$

$$\implies \frac{dh}{dx} = I_1 \frac{3}{2}c^2 \approx 1.8 \quad (4.20)$$

the leading order streamwise momentum equation gives a constant slope for the free surface.

4.4. Depth-integrated wall-normal momentum

We integrate (4.8) across the film to obtain

$$\frac{d}{dx} \int_0^h uw dz = p(0) + h'' - 2 \partial_z w|_{z=h} + [\partial_z w]_0^h. \quad (4.21)$$

Substituting equations (4.14) and (4.16) for velocity, we find

$$\int_0^h uw dz = u_s^2 h h' I_2, \quad I_2 := \int_0^1 \eta f(\eta)^2 d\eta \approx 0.339, \quad (4.22)$$

$$\partial_z w|_{z=h} = \frac{u_s h'}{h}, \quad \partial_z w|_{z=0} = 0. \quad (4.23)$$

Using $u_s = 1/(I_1 h)$ from (4.15) gives

$$\frac{d}{dx} \int_0^h uw dz = \frac{I_2}{I_1^2} \frac{d}{dx} \left(\frac{h'}{h} \right) = \frac{I_2}{I_1^2} \left(\frac{h''}{h} - \frac{h'^2}{h^2} \right), \quad (4.24)$$

$$\partial_z w|_{z=h} = \frac{h'}{I_1 h^2}. \quad (4.25)$$

Substituting into (4.21) and writing $P_0 := p(0)$ yields the film-height ODE

$$h'' = \frac{\frac{I_2}{I_1^2} \frac{h'^2}{h^2} - \frac{h'}{I_1 h^2} + P_0}{\frac{I_2}{I_1^2} \frac{1}{h} - 1} \quad (4.26)$$

Equation (4.26) shows an apparent singularity when $\frac{I_2}{I_1^2} \frac{1}{h} = 1$ however, this singularity must be regularised by the wall pressure P_0 , a Lagrange multiplier enforcing incompressibility.

We revisit the scaled form of the denominator, which can be written as,

$$\frac{I_2}{I_1^2} \frac{1}{h^*} \equiv I_2 u_s^{*2} h^* We \equiv I_2 \frac{\rho u_s^2 h}{\sigma}. \quad (4.27)$$

$I_2 \frac{\rho u_s^2 h}{\sigma}$ can also be defined as the local Weber number. Confirming the wave argument; equation (4.27) shows the shock at the location where the local weber number reaches unity. Hence, we divide the flow that is connected by a jump or a shock into two regimes,

$$\frac{I_2}{I_1^2} \frac{1}{h^*} = \begin{cases} > 1, & \text{Supercritical} \\ < 1, & \text{Subcritical} \end{cases} \quad (4.28)$$

4.5. Comparison with the standing wave result

In equation (2.7), we set U as the average velocity of the film. We compare Equation (2.7) with (4.27) to find the value of ψ to get

$$\psi = \frac{I_1}{\sqrt{I_2}} \approx 1. \quad (4.29)$$

5. Results

Solving the film-height evolution equation (4.26) requires knowledge of the pressure field. Our leading-order analysis demonstrated that the streamwise pressure gradient $\partial_x p$ is $\mathcal{O}(\epsilon^2)$; thus, within the slowly varying thin-film region, the pressure may be approximated as constant. However, this assumption holds only in the outer region and breaks down near the jump, where pressure gradients become significant to regularise the flow. Consequently, we distinguish between the outer free-surface flow, where $p \approx \text{const}$, and the inner jump region, where the pressure P_0 effectively varies to enforce continuity.

With $\mathcal{H} \equiv h'$, the depth-integrated model reduces to a dynamical system:

$$h' = \mathcal{H}, \quad \mathcal{H}' = \frac{N(h, \mathcal{H})}{D(h)}, \quad (5.1)$$

$$N(h, \mathcal{H}) = \frac{I_2}{I_1^2} \frac{\mathcal{H}^2}{h^2} - \frac{1}{I_1} \frac{\mathcal{H}}{h^2} + P_0, \quad (5.2)$$

$$D(h) = \frac{I_2}{I_1^2} \frac{1}{h} - 1. \quad (5.3)$$

The phase-space structure can be determined by the nullclines obtained by setting $N(h, \mathcal{H}) = 0$ and $D(h) = 0$. One boundary condition is provided by the similarity slope (4.20), while the second depends on the initial film height.

The system (5.1)–(5.3) exhibits a critical singularity when the denominator $D(h)$ vanishes, corresponding to the critical Weber number condition derived in §4.1. The apparent singularity gives an impression of a breakdown of the model or a shock. However, in the full viscous system, the pressure is not merely a passive variable but acts as a degree of freedom. Specifically, the wall pressure P_0 (and its gradient) functions as the *Lagrange multiplier* that enforces the incompressibility constraint.

We hypothesise that when the flow approaches the singularity ($We \rightarrow 1$), the constraint of mass conservation forces the pressure gradient to adjust, thereby regularising the equation. This adjustment allows the flow to negotiate the transition from the supercritical thin film ($We > 1$) to the subcritical downstream layer ($We < 1$) through a smooth, albeit rapid, variation in depth—the hydraulic jump. Thus, while the depth-averaged scaling predicts a singularity at $We = 1$, the complete pressure field resolves it, ensuring a continuous physical solution.

6. Conclusions

We have presented a theoretical framework for planar hydraulic jumps where surface tension acts as the primary control mechanism. By analysing the gravity-capillary dispersion relation, we showed that even for inviscid fluids, capillarity can in principle set hydraulic control, resulting in the hydraulic jump.

We then analysed the viscous shallow-water equations in the zero-gravity limit and demonstrated that the deviatoric component of normal stress plays a leading-order role in the thin-film momentum balance—a contribution often neglected in classical shallow-water theory.

Our dominant-balance analysis identifies a critical singularity where the local Weber number reaches unity ($We = 1$), analogous to the Froude number condition in gravity-driven flows. We have shown that this singularity corresponds to the location where the mean flow velocity matches the speed of the fastest admissible capillary wave (the zero-mode), providing a robust criterion for hydraulic control. Furthermore, our analysis suggests that the apparent singularity in the depth-averaged equations is regularised by the pressure field, which acts as a Lagrange multiplier to enforce continuity across the jump. These results establish that surface tension alone is sufficient to pin a hydraulic jump in thin films, challenging the classical gravity-centric view.

Acknowledgements

I would like to express my sincere gratitude to Prof. Paul Linden and Dr. Amir Atufi for their stimulating discussions and suggestions.

Appendix A. Viscous cutoff (order-of-magnitude)

Very short capillary waves are attenuated by viscosity. Balancing the decay rate $\sim \nu k^2$ with the capillary frequency $\omega \sim [(\sigma/\rho)k^3]^{1/2}$ gives $k_\nu \sim \sigma/(\rho \nu^2)$. For water ($\sigma \approx 0.072 \text{ N m}^{-1}$, $\rho \approx 10^3 \text{ kg m}^{-3}$, $\nu \approx 10^{-6} \text{ m}^2 \text{ s}^{-1}$) this yields $k_\nu \sim 7 \times 10^7 \text{ m}^{-1}$ ($\lambda \sim 90 \text{ nm}$), far beyond the long-wave range and irrelevant to the control criterion.

The Influence of surface tension in hydrodynamics

REFERENCES

BALMFORTH, NEIL J & MANDRE, S 2004 Dynamics of roll waves. *Journal of Fluid Mechanics* **514**, 1–33.

BHAGAT, RAJESH K, JHA, NK, LINDEN, PF & WILSON, D IAN 2018 On the origin of the circular hydraulic jump in a thin liquid film. *Journal of Fluid Mechanics* **851**, R5.

BHAGAT, RAJESH K & LINDEN, PAUL F 2020 The circular capillary jump. *Journal of Fluid Mechanics* **896**, A25.

BHAGAT, RAJESH K, WILSON, D IAN & LINDEN, PF 2020 Experimental evidence for surface tension origin of the circular hydraulic jump. *arXiv preprint arXiv:2010.04107*.

BOHR, TOMAS, DIMON, PETER & PUTKARADZE, VAKHTANG 1993 Shallow-water approach to the circular hydraulic jump. *Journal of Fluid Mechanics* **254**, 635–648.

BUSH, JOHN WM & ARISTOFF, JEFFREY M 2003 The influence of surface tension on the circular hydraulic jump. *Journal of Fluid Mechanics* **489**, 229–238.

DHAR, MRINMOY, DAS, GARGI & DAS, PRASANTA KUMAR 2020 Planar hydraulic jumps in thin film flow. *Journal of Fluid Mechanics* **884**, A11.

DUCHESNE, ALEXIS & LIMAT, LAURENT 2022 Circular hydraulic jumps: where does surface tension matter? *Journal of Fluid Mechanics* **937**, R2.

JANNES, GIL & ROUSSEAU, GERMAIN 2012 The circular jump as a hydrodynamic white hole. *arXiv preprint arXiv:1203.6505*.

KURIHARA, M 1946 On hydraulic jumps. *Proceedings of the Report of the Research Institute for Fluid Engineering, Kyusyu Imperial University* **3** (2), 11–33.

MARUSIC, IVAN & BROOMHALL, SUSAN 2021 Leonardo da vinci and fluid mechanics. *Annual Review of Fluid Mechanics* **53** (1), 1–25.

RAZIS, DIMITRIOS, KANELLOPOULOS, GIORGOS & VAN DER WEELE, KO 2021 Continuous hydraulic jumps in laminar channel flow. *Journal of Fluid Mechanics* **915**, A8.

TANI, ITIRO 1949 Water jump in the boundary layer. *Journal of the Physical Society of Japan* **4** (4–6), 212–215.

WATSON, EJ 1964 The radial spread of a liquid jet over a horizontal plane. *Journal of Fluid Mechanics* **20** (3), 481–499.